BUCKLING BEHAVIOR OF COMPOSITE FERROCEMENT PLATES

Apostolos Koukouselis
Civil Engineer, M.Sc., Doctoral Candidate
Laboratory of Structural Analysis and Design, Department of Civil Engineering, University of Thessaly
Volos, Greece
e-mail: akoukouselis@gmail.com

Euripidis Mistakidis
Professor
Laboratory of Structural Analysis and Design, Department of Civil Engineering,
University of Thessaly, Volos, Greece
e-mail: emistaki@uth.gr

1. SUMMARY

Ferrocement is a type of reinforced concrete using closely spaced multiple layers of mesh and/or small diameter steel rods, completely infiltrated with, or encapsulated, in mortar. One of its most common applications is the manufacturing of shells and plates of small thickness, which are prone to buckling. Besides the geometrical nonlinearity, the effect of cracking causes great material nonlinearities, further complicating the study of such structures. In this paper the behavior of a slender ferrocement plate stiffened by a grid of I-profile steel beams, is investigated through detailed three-dimensional finite element models. The composite ferrocement plate, which consists of a repeating 5x5 m base unit, is subjected to in plane axial loading. Four cases are investigated regarding the thickness of the skin, 20mm, 25mm, 30mm and 35mm respectively. Following the guidelines of the relevant Eurocodes, first a linear buckling analysis is performed that, besides providing the elastic buckling capacity of the plate, also helps determine the boundary conditions that must be applied at the base 5x5 m unit in order to reduce the size of the model. Then, a set of geometrically and materially nonlinear analyses with initial imperfection according to the predominant buckling shapes, as calculated by the buckling analysis, provide the ultimate axial load carrying capacity of the structure.

2. INTRODUCTION

Ferrocement, as defined by the ACI committee 549 [1], is a form of reinforced concrete that uses as reinforcement multiple layers of closely spaced steel meshes of small diameter. As

ferrocement is the predecessor of conventional reinforced concrete (R/C) there are many similarities between the two materials and the general guidelines and standards regarding R/C structures also apply in the ferrocement ones. However, the distinct differences in their behavior should be taken into account during the analysis and design of such elements. As Naaman [2] mentions, in contrast to R/C, ferrocement elements are usually of small thickness (15 to 25mm). Reinforcement is distributed throughout the thickness in both directions, with typical reinforcement ratios that are a lot higher than those of conventional reinforced elements (2- 8 % total or 1 – 4 % in each direction). These facts lead to elements with high tensile strength (of the same order as the compressive one), high ductility that, unlike in R/C elements, increases with the increase of the reinforcement ratio, homogeneous-isotropic properties in two directions and high punching shear resistance.

Due to the above mechanical characteristics one of its most common applications is the manufacturing of shells and plates of small thickness used as facade and roofing systems. In many cases ferrocement elements are not just architectural free-form decorative elements but are also a part of the structural system. In these cases the shells and plates are usually stiffened as they are called to carry substantial in and out of plane loads. However, due to the small thickness of the skin buckling failure may occur. Moreover, besides the geometrical nonlinearity, the intrinsic issues of cracking in cementitious composites, cause great material nonlinearities to arise making the study of such structures even more complicated.

In this study such a stiffened plate structure prone to buckling is investigated. The stiffeners are considered to be steel I-profile beams while the skin of the plate is considered to have a variable thickness ranging from 20 to 35mm. As nowadays detailed guidelines and regulations regarding ferrocement structures do not exist, the analysis is based on the general provisions of the relevant regulations, such as Eurocode 2 and 3 [3][4][5][6], which involve both materially and geometrically nonlinear analysis. Section 3 describes the structure under investigation, the formulation of the numerical model and the analysis procedure. Section 4 summarizes the properties of the materials used in the analyses of the structure, while Section 5 demonstrates the results of the analyses. Finally, Section 6 provides a discussion of the results and the conclusions of the investigation.

3. THE STRUCTURE UNDER INVESTIGATION

The structure under investigation is a ferrocement plate stiffened by the means of a grid of steel beams. The plate consists of a repeating 5x5 m base unit, the geometry of which is shown in Figure 1, and is supported in a rhomboid pattern every 2.5 m. Along the *x* direction the plate is stiffened by a HEB160 beam every 2.5 m while along the *y* direction a IPE160 stiffener exists every 1.25 m. Four cases regarding the thickness of the plates were investigated, 20, 25, 30 and 35 mm respectively. The reinforcement of the skin comes in the form of steel meshes. Figure 2 shows the reinforcement pattern of the cases investigated.

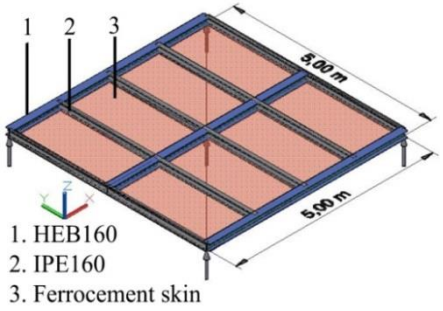

Figure 1. Base 5x5 m unit.

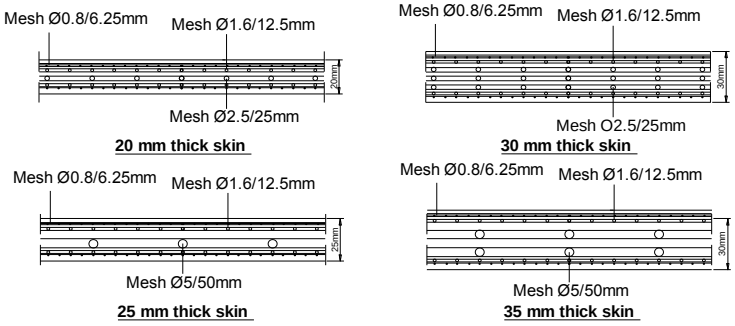

Figure 2. Reinforcement patterns.

The elastic-plastic resistance of the structure was determined by a FEM analysis. The relevant regulations for such analyses are included in Annex C of EN1993-1-5 [5] and §8.7 of EN1993-1-6 [6], depending on whether the structure is a plate or a shell. The methodologies described in the framework of the two regulations are similar and involve a series of linear buckling analyses (LBA) and geometrically and materially nonlinear analyses of the imperfect structure (GMNIA) and the only significant difference is found on the amplitude of the assumed initial imperfections. The LBA is used to determine the elastic critical load as well as the shape of the initial imperfections for the GMNIA. In this study, as the structure consists of a repeating 5x5 m unit, the LBA is also used in order to determine the boundary conditions that apply on the edges of this base unit (symmetry or antisymmetry) so that the computational model is reduced.

The structure was modelled and analyzed through the nonlinear FE analysis software MSC Marc [7], using four-node thick shell elements. For the nonlinear analysis, the reinforced ferrocement skin was modelled by the use of composite layered shells rather than by the use of the more traditional method of combining shell and beam elements, as the first modelling technique has many advantages. First, there are less mesh limitations as, in contrast to the later modelling method, there is no need for beam elements simulating the reinforcement rods and shell elements representing the matrix to be combined at common nodal points. Next, the position of the reinforcement layers can be accurately and easily simulated with no need of introducing beam offsets or rigid links and thus the bending behavior of the ferrocement skin can be captured efficiently. The layers representing the matrix are isotropic while the ones representing the reinforcement meshes are orthotropic with stiffness only along the direction of the rods they represent. The models were solved using a Full Newton- Raphson iterative procedure and the convergence testing was based on the residual forces.

4. MATERIAL PROPERTIES FOR THE ANALYSES

The matrix of the ferrocement skin was assumed to be a cementitious mortar with strengths similar to those of grade C60/75 concrete. For the needs of the nonlinear numerical analysis, the material behavior was based on the recommendations of EN1992-1-1 §3.1.5 [3], taking into consideration the provisions of §5.8.6(3) regarding nonlinear second order analysis. The design values for the ultimate compressive and tensile strength were used ($f_{cd} = 40$ MPa,

$f_{ctd} = 2.066$ MPa) thus, the design axial capacity can be directly calculated. As §5.8.6(3) suggests, the modulus of elasticity E_{cm} was reduced by the material partial factor on the elastic modulus for buckling analysis $\gamma_{cE} = 1.2$ resulting to a design value for modulus of elasticity $E_{cd} = E_{cm}/\gamma_{cE}$ equal to 32.5 GPa.

The material properties of the grade B500c reinforcing steel were based on the provisions of EN1992-1-1 [3]. The behavior of the material was considered to be elastic perfectly plastic with a yield plateau at 435 MPa and the modulus of elasticity was considered to be 200 GPa. It should be reminded that the material representing the reinforcement layers was considered orthotropic with stiffness only along the direction of the reinforcing rods as the modelling technique by composite layered shell demands.

The material properties for the used S235 structural steel were based on EN1993-1-1 [4]. The material was considered isotropic with an elastic-perfectly plastic behavior without strain hardening. The modulus of elasticity E was considered to be equal to 210 GPa, while the design value of the yield stress f_{yd} was taken equal to 235 MPa.

5. RESULTS

5.1 Linear Buckling Analysis

For the LBA, the loading was imposed as "edge load" on the edges of the outer shell elements in such a way that load eccentricities are minimized. Originally, a 15x15m model with the central 5x5m region loaded was analyzed. The outer spans provide stability and prevent the development of misleading buckling modes localized at the edges of the model. After the determination of the predominant buckling mode by the 15x15m model, a 5x5 model with proper boundary conditions on its edges was analyzed, as it is common in similar research [8]. As mentioned in the relevant literature [9], the main buckling modes of the stiffened plates are local, global and mixed ones. Figure 3 presents the buckling modes produced by the linear buckling analysis of the four cases investigated in this study as well as the boundary conditions that were applied at the edges of the 5x5 m unit. Table 1 summarizes the results of the above numerical analyses regarding the buckling modes and loads.

Plate thickness	Loading direction	Mode	15x15m model (kN/m)	5x5m model (kN/m)	Plastic axial capacity (kN/m)
20mm	*x*	Local	815	556,9	1570
20mm	*y*	Local	1772.5	1235	1435
25mm	*x*	Local	1358	905.1	1847
25mm	*y*	Local	3092	2103	1712
30mm	*x*	Local	2101	1380	2125
30mm	*y*	Global	-*	2981	1990
35mm	*x*	Local	3070	2061	2402
35mm	*y*	Global	7160 *	3236	2267

* Due to the presence of the outer spans a local buckling mode arises.

Table 1. Buckling modes and loads.

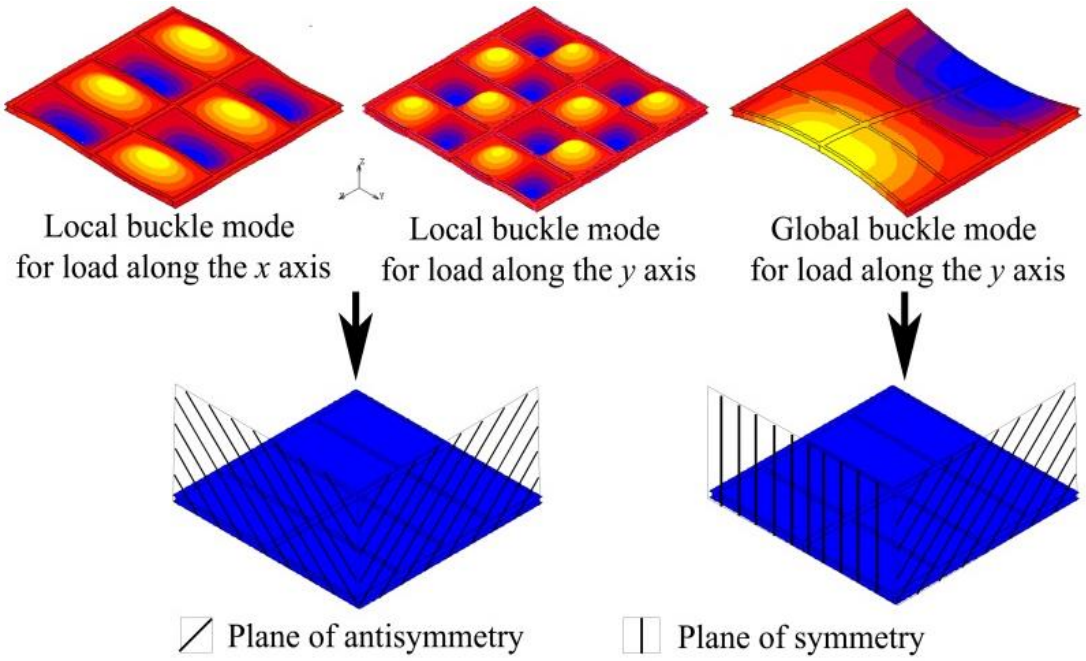

Figure 3. Buckling modes and corresponding boundary conditions.

5.1 Geometrically and materially nonlinear analysis

Having determined the predominant buckling modes (local and global) as well as the boundary conditions that apply on the 5x5 m base unit, imperfections were incorporated at the initial geometry of the model according to the buckling shape. EN1993-1-5 [5] recommends the maximum magnitude of the initial imperfections (out of plane) to be $l/200$, resulting to 25mm for the global mode and 12.5mm for the local one. As the weak *x* axis has a lower load carrying capacity, the nonlinear analysis is focused on this direction.

In order to capture the post-buckling response, the analyses have to be displacement controlled. Thus, the loading was imposed in the form of axial displacement along the first internal plane of symmetry, reducing the model to 3.75x5 m ("Type 1" analysis). As this analysis allows the redistribution of the load after the buckling of the skin, a second type of analysis was carried out on the 5x5 m model that was load controlled ("Type 2" analysis). Finally, as after the buckling of the skin a global failure mode is possible, a third 5x5 m model was analyzed ("Type 3" analysis) that had boundary conditions corresponding to the global buckling mode and both local and global imperfections (12.5 and 25mm respectively). Figures 4 to 7 demonstrate the response of the four stiffened plates. In "Type 1" analyses the models reach axial loads well above the elastic local buckling due to the fact that after the buckling of the plate, the structure still has the ability to undertake further loading through the stiffeners. Figure 8 demonstrates the reaction of the nodes of the loaded edges at different increments. After a certain point the skin buckles losing its ability to carry additional loads and thus any extra load is carried thought the stiffeners. In "Type 2" analyses (load controlled) load redistribution cannot take place, therefore the structure cannot undertake any extra load after the buckling of the skin. Finally, in "Type 3" analyses, the structure buckles locally and then

passes to a stable post-buckling path until it fails due to the yielding of the stiffeners and not due to global buckling.

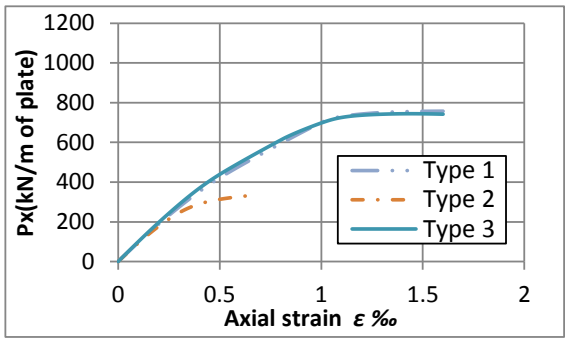

Figure 4. Response of the 20mm thick plate along the *x* axis.

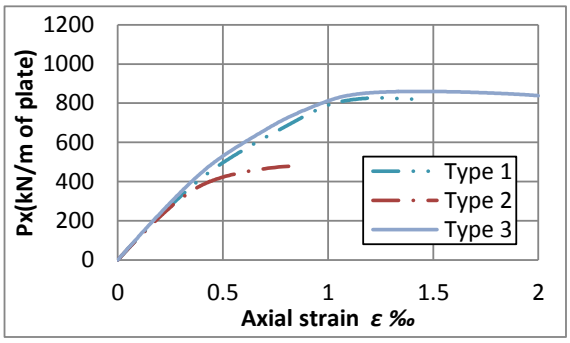

Figure 5. Response of the 25mm thick plate along the *x* axis.

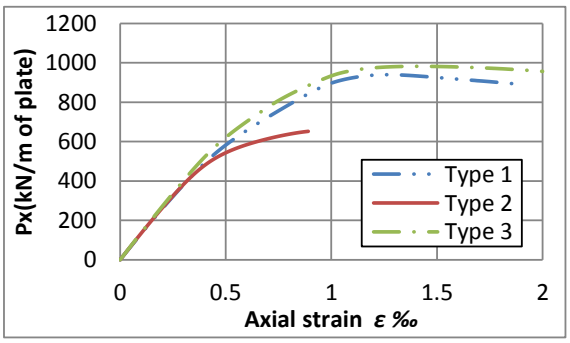

Figure 6. Response of the 30mm thick plate along the *x* axis.

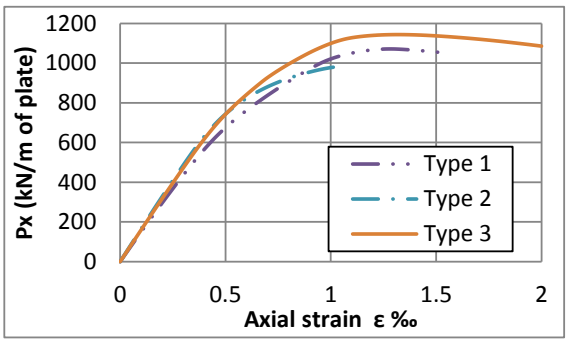

Figure 7. Response of the 35mm thick plate along the *x* axis.

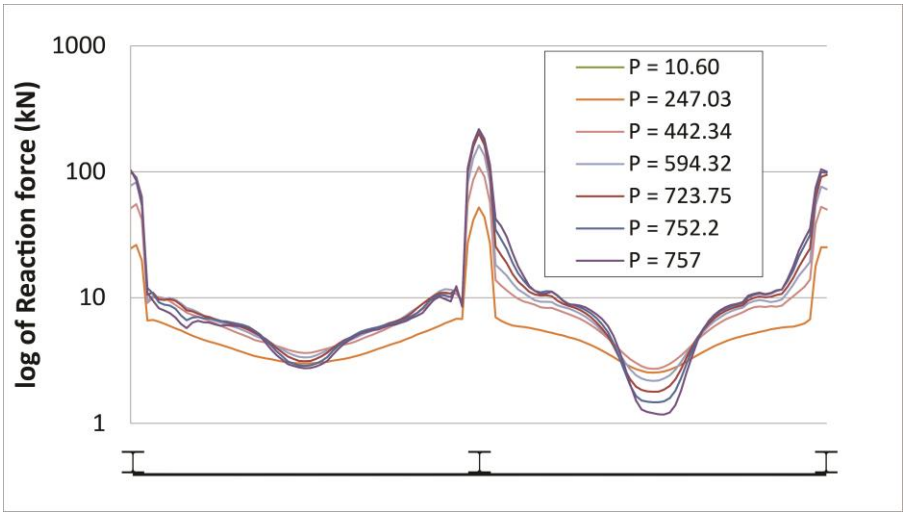

Figure 8 Distribution of the reaction force along the edge of the skin.

6. DISCUSSION AND CONCLUSIONS

The analysis of the structure at hand identified that two are the predominant buckling modes: local buckling of the ferrocement skin between the steel stiffeners, and global buckling of the whole structure between out of plane supports. Table 1 demonstrates that local buckling results in lower elastic buckling loads, below the axial plastic load carrying capacity of the stiffened plate. The geometrically and materially nonlinear analysis of the structure however, demonstrates the ability of the structure to carry load beyond the load corresponding to the local buckling of the skin, through stress redistribution. If full load redistribution can develop, the plate can still carry load after the buckling of the ferrocement skin, reaching about 44% of its axial capacity, as was the case in all four thicknesses investigated. The aforementioned load corresponds to the combination of the elastic-plastic buckling resistance of the skin and the plastic compression capacity of the steel stiffeners. In cases were the aforementioned redistribution mechanism cannot develop, caution is needed by the designer as the ultimate axial load of the structure drops to the elastic-plastic buckling resistance of the skin. Moreover, special care should be given to the satisfaction of the serviceability criteria, as after the buckling of the skin the out of plane displacements may be beyond the acceptable range. Finally, the set of analysis with global buckling boundary conditions and both local and global boundary conditions demonstrated that no significant interaction between local and global buckling appears, and in some cases the above analyses led to a higher ultimate strength of the structure, possibly due to the high initial imperfection sensitivity of the problem at hand.

7. REFERENCES

[1] ACI Committee 549, "ACI 549.1R-93 Guide for the Design, Construction, and Repair of Ferrocement", Reapproved 1999.

[2] Naaman A. E., "Ferrocement and Laminated Cementitious Composites", Techno Press 3000, Ann Arbor, Michigan, USA, 2000.

[3] EN1992-1-2, "Eurocode 2: Design of concrete structures - Part 1-1: General rules and rules for buildings", Brussels, 2004.

[4] EN1993-1-1, "Eurocode 3: Design of steel structures - Part 1-1: General rules and rules for buildings", Brussels, 2005.

[5] EN1993-1-5, "Eurocode 3: Design of steel structures - Part 1.5 : Plated structural elements", Brussels, 2006.

[6] EN1993-1-6, "Eurocode 3: Design of steel structures Part 1-6 : Strength and Stability of Shell Structures", Brussels, 2007.

[7] MSC Marc, "MSC Marc, Volume A: Theory and user information", MSC Software Corporation, USA, 2011.

[8] Mittelstedt C., "Explicit local buckling analysis of stiffened composite shells accounting for periodic boundary conditions and stiffener–shell interaction", *Composite Structures*, Vol. 91, No. 3, pp. 249-265, 2009.

[9] Stamatelos D.G., Labeas G.N., Tserpes K.I., "Analytical calculation of local buckling and post-buckling behavior of isotropic and orthotropic stiffened panels", *Thin-Walled Structures*, Vol. 49, pp. 422-430, (2011).

ΛΥΓΙΣΜΙΚΗ ΣΥΜΠΕΡΙΦΟΡΑ ΣΥΜΜΙΚΤΩΝ ΠΛΑΚΩΝ ΑΠΟ FERROCEMENT

Απόστολος Κουκουσέλης
Πολιτικός Μηχανικός, M.Sc., Υποψήφιος Διδάκτωρ
Εργαστήριο Ανάλυσης και Σχεδιασμού Κατασκευών, Τμήμα Πολιτικών Μηχανικών,
Πανεπιστήμιο Θεσσαλίας, Βόλος, Ελλάδα
e-mail: akoukouselis@gmail.com

Ευριπίδης Μυστακίδης
Καθηγητής
Εργαστήριο Ανάλυσης και Σχεδιασμού Κατασκευών, Τμήμα Πολιτικών Μηχανικών,
Πανεπιστήμιο Θεσσαλίας, Βόλος, Ελλάδα
e-mail: emistaki@uth.gr

ΠΕΡΙΛΗΨΗ

Το ferrocement είναι ένας τύπος οπλισμένου σκυροδέματος που αποτελείται από πολλαπλές οπλισμικές στρώσεις χάλυβα μικρής διαμέτρου, που είναι πλήρως εγκιβωτισμένες σε κονίαμα. Μια από της πιο συνηθισμένες εφαρμογές του ferrocement είναι στην κατασκευή λεπτών κελυφών και πλακών που είναι επιρρεπείς σε λυγισμό. Εκτός από τη γεωμετρική μη γραμμικότητα, το φαινόμενο της ρηγμάτωσης προκαλεί έντονη μη γραμμική συμπεριφορά του υλικού, δυσχεραίνοντας ακόμη περισσότερο την μελέτη αυτών των κατασκευών. Στη παρούσα εργασία μελετάται μέσω τρισδιάστατων λεπτομερών μοντέλων πεπερασμένων στοιχείων μια τέτοια λυγηρή πλάκα από ferrocement, ενισχυμένη και στις δυο διευθύνσεις από σχάρα μεταλλικών δοκών διατομής διπλού Τ. Η σύμμεικτη πλάκα, που αποτελείται από μια επαναλαμβανόμενη μονάδα 5x5m, υπόκειται σε εντός επιπέδου αξονικό φορτίο. Μελετώνται τέσσερις περιπτώσεις σχετικά με το πάχος της πλάκας, 20 χιλ., 25 χιλ., 30 χιλ. και 35 χιλ. αντίστοιχα. Ακολουθώντας τις οδηγίες των σχετικών Ευροκωδίκων, αρχικά πραγματοποιείται γραμμική ανάλυση λυγισμού η οποία, εκτός από το να προσφέρει το ελαστικό φορτίο λυγισμού, βοηθάει στον προσδιορισμό των συνοριακών συνθηκών που πρέπει να εφαρμοστούν στα άκρα της βασικής 5x5 μονάδας ώστε να μειωθεί το μέγεθος του υπολογιστικού μοντέλου για την εφαρμογή των μη-γραμμικών αναλύσεων. Ακολούθως, μέσω μιας σειράς μη γραμμικών αναλύσεων με αρχικές ατέλειες σύμφωνα με την δεσπόζουσα ιδιομορφή λυγισμού, όπως αυτή υπολογίστηκε από την ανάλυση λυγισμού, προσδιορίζεται η μέγιστη αξονική αντοχή της κατασκευής.